

Nanoscale Push–Push Dihydrophenanthrene Derivatives as Novel Fluorophores for Two-Photon-Excited Fluorescence**

Lionel Ventelon, Sandrine Charier, Laurent Moreaux, Jerome Mertz, and Mireille Blanchard-Desce*

Molecular two-photon absorption (TPA)^[1] has gained interest over recent years owing to its applications in various fields, including spectroscopy, optical data storage,^[2] optical power limitation,^[3] and microfabrication.^[4] Among these, two-photon-excited fluorescence (TPEF) has gained widespread popularity in the biological community and has given rise to the technique of two-photon laser scanning fluorescence microscopy.^[5] In standard fluorescence microscopy, molecular excitation is caused by the absorption of a single photon. Molecular excitation by the simultaneous absorption of two photons, however, presents several advantages including a capacity for a highly confined excitation and intrinsic three-dimensional resolution, and the possibility of imaging at an increased penetration depth in tissue, with reduced photo-damage and background fluorescence.^[5b] TPEF microscopy was initially developed by using conventional fluorophores whose TPA characteristics were not optimized and thus led to the necessity of high laser intensities and/or fluorophore concentrations. It has become clear that the development of TPEF microscopy would greatly benefit from the design of novel fluorophores specifically engineered for efficient TPEF. Key features for such a purpose are large TPA cross sections σ_2 and a high fluorescence quantum yield Φ . We present herein the design, synthesis, and potential applications for membrane imaging of a series of novel fluorophores that demonstrate enhanced TPEF cross sections in the visible-red or near-IR region.

It has been observed recently that symmetrical conjugated molecules that bear two electron-donating D (or electron-withdrawing A) end groups can display high nonlinear absorption characteristics^[3] and large σ_2 values.^[6] Such behavior is correlated to an intramolecular charge redistribution that occurs between the ends and the center of the molecule. Enhancing this quadrupolar charge transfer, either

in D-AA-D or A-DD-A derivatives,^[7] or by lengthening the conjugated system,^[6b,c] can lead to significant increases in σ_2 . Unfortunately, this often leads to a decrease in the fluorescence quantum yield. Based on these observations, our aim has been to design elongated systems that display large σ_2 in the visible-red/NIR region (700–900 nm), while maintaining high fluorescence quantum yields. Our molecular-engineering strategy is based on the push–push (e.g. bis-donor) functionalization of a semirigid nanoscale conjugated system. The structure is built from the symmetrical grafting of two elongated rods that bear a donating end group on a rigid conjugated core (Figure 1).

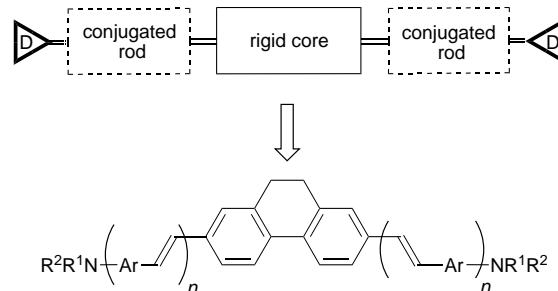


Figure 1. Molecular engineering of push–push fluorophores with high two-photon absorptivity. Based on earlier work,^[6a] the dihydrophenanthrene moiety was chosen as the central building block. The extending rods were built from arylene–vinylene oligomers which were expected to ensure electronic conjugation and maintain acceptable fluorescence quantum yields. The di(*n*-alkyl)amino substituents act both as donors and as solubilizing end groups.

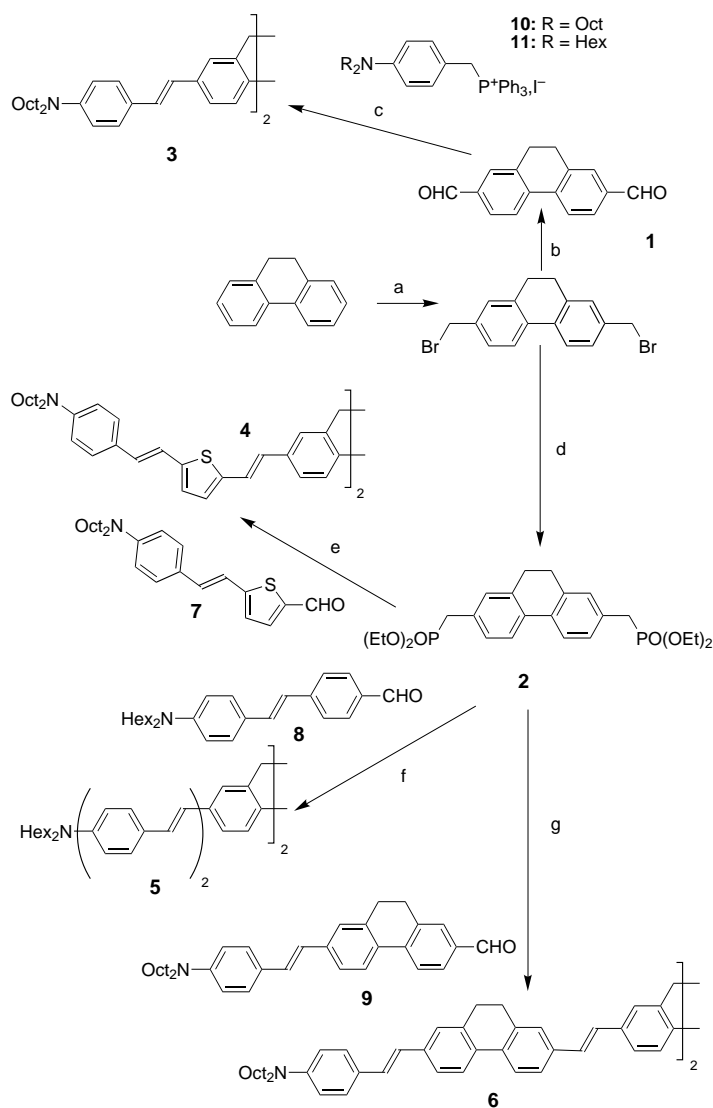
Based on this strategy, we have prepared push–push molecules with a conjugation length that varies from 23 Å to 44 Å (Scheme 1). These compounds were synthesized from symmetrical reagents derived from dihydrophenanthrenes **1** and **2**. Push–push molecule **3** was readily obtained in one step from bisaldehyde **1**^[8] in 70% yield by means of a double Wittig reaction. Push–push molecules **4**–**6** were prepared from bisphosphonate **2** in yields of 71%, 94%, and 64%, respectively, by means of a double Wittig–Horner condensation with conjugated aldehydes **7**–**9**. The conjugated aldehyde **7** was prepared by treating 2,5-thiophenebiscarboxaldehyde with one equivalent of phosphonium reagent **10**. Similarly, **8** was obtained from terephthalaldehyde *mono*-(diethyl acetal) and one one equivalent of **11**, while the reaction of bisaldehyde **1** and **10** afforded the conjugated aldehyde **9**. The core reagent **2** was synthesized from dihydrophenanthrene in a two-step procedure by double bromomethylation^[8] followed by a Michaelis–Arbusov reaction.

The TPA cross sections of molecules **3**–**6** were determined by comparing their TPEF to that of fluorescein.^[9, 10] This procedure provides the TPEF action cross section, defined by $\sigma_2\Phi$. The corresponding σ_2 values can be derived by independently determining the fluorescence quantum yield Φ from standard fluorescence measurements (Table 1).^[11] Molecules **3**–**6** indeed combine very large two-photon absorption cross sections in the visible-red region and high fluorescence quantum yields. All new fluorophores outperform the standard fluorophore fluorescein by more than one or two orders

[*] Dr. M. Blanchard-Desce
Synthèse et Electrosynthèse Organiques (CNRS, UMR 6510)
Université de Rennes 1
Campus Scientifique de Beaulieu, Bât. 10A, 35042 Rennes (France)
Fax: (+33)2-99-28-62-77
E-mail: mireille.blanchard-desce@univ-rennes1.fr
L. Ventelon, S. Charier
Département de Chimie, Ecole Normale Supérieure, 24, rue Lhomond, 75231 Paris Cedex 05 (France)
L. Moreaux, Dr. J. Mertz
Neurophysiologie et Nouvelles Microscopies (INSERM EPI 00-02)
Ecole Supérieure de Physique et Chimie Industrielle
rue Vauquelin 10, 75231 Paris Cedex 05 (France)

[**] This work was supported by the Délégation Générale pour l'Armement (DGA), the Institut Curie, and the Centre National de la Recherche Scientifique (CNRS). L.V. and L.M. received fellowships from the DGA and CNRS, respectively.

Supporting information for this article is available on the WWW under <http://www.angewandte.com> or from the author.



Scheme 1. a) $(\text{CH}_2\text{O})_3$, HBr, H_3PO_4 , 24 h, 90 °C; b) NaHCO_3 , DMSO, 4 h, 115 °C; c) **10** (2.1 equiv), $t\text{BuOK}$ (3 equiv), [18]crown-6, CH_2Cl_2 , 5 h, RT; d) $\text{P}(\text{OEt})_3$ (3 equiv), 6 h, 150 °C; e)–g) **7**, **8**, or **9** (2.1 equiv), respectively, NaH (3 equiv), [18]crown-6, THF, 16 h, RT.

Table 1. One-photon and two-photon absorption and fluorescence properties of molecules **3**–**6** in solution.

	l nm ^[a]	$\lambda_{\text{max}}(\text{abs})$ nm ^[b]	$\lambda_{\text{max}}(\text{em})$ nm ^[c]	Φ^{d}	$\sigma\Phi$ [GM] ^[e]	σ_2 [GM] ^[e]
Fluorescein		490	514	0.9 ^[11]	27 ^[10]	30 ^[10]
3 ^[f]	2.3	410	456	0.86	1490	1730
4 ^[f]	3.4	465	521	0.52	1330	2560
5 ^[f]	3.5	428	477	0.82	1870	2270
5 ^[g]	3.5	428	522	0.60	1980	3310
6 ^[g]	4.4	422	514	0.66	2480	3760

[a] Length of the push–push extended system evaluated by molecular mechanics calculation of the maximum distance between the nitrogen atoms of the donating end groups. [b] Absorption maxima. [c] Emission maxima. [d] Fluorescence quantum yield determined relative to fluorescein. [e] Values given at 740 nm in GM; 1 GM = $10^{-50} \text{ cm}^4 \text{ s photon}^{-1}$. [f] In toluene. [g] In chloroform.

of magnitude. As indicated by the comparison of molecules **3** and **5**, an increase in the length of the phenylene-vinylene oligomeric extending rods results in a noticeable increase in the TPA cross section while maintaining a nearly constant

quantum fluorescence yield. As a result, a net increase in the TPEF action cross section in the visible-red region is obtained. The effect of increasing length is also observed when a phenylene unit is substituted by a dihydrophenanthrene unit in the arylene-vinylene oligomers: fluorophore **6** combines a larger TPA cross section and quantum fluorescence yield than fluorophore **5**, while being slightly blue-shifted. As a result, fluorophore **6** shows both large TPA (with $\sigma_2 = 4200 \times 10^{-50} \text{ cm}^4 \text{ s photon}^{-1}$ at 710 nm) and TPEF cross sections in the visible-red region. An increase in the conjugation length also induces a significant broadening of the TPEF spectra in the NIR region (Figure 2a). Whereas molecule **3** shows a steeply declining TPEF cross section above 750 nm, fluorophores **5** and **6** maintain high TPEF cross sections in the 750–850 nm region (Figures 2a and b). The lowest energy TPA peaks are observed at higher energy than twice that corresponding to one-photon absorption maxima (Table 1). This is consistent with a higher lying TPA-allowed electronic excited state responsible for high

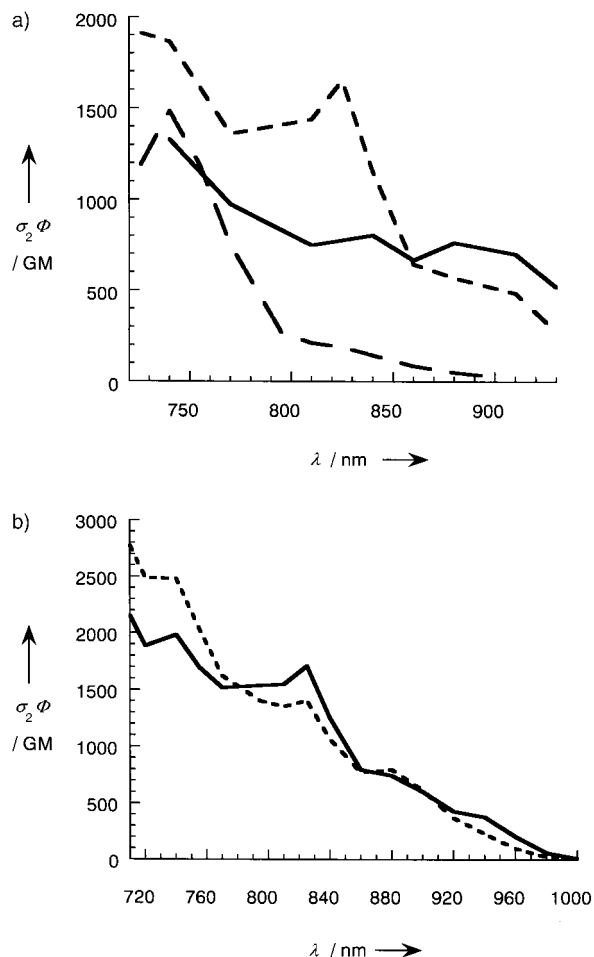


Figure 2. a) TPEF action cross sections of fluorophores **3**–**5** in toluene: **3** (---), **4** (—), **5** (---). b) TPEF action cross sections of fluorophores **5**–**6** in chloroform: **5** (—), **6** (---). Solutions of fluorophores **3**–**6** diluted to a final concentration of approximately 100 μM were used. TPEF measurements were calibrated relative to the absolute TPEF action cross section for fluorescein in water (pH 11).^[9,10] For each data point, an additional control was performed by comparing with the TPEF action cross section of rhodamine B in methanol.^[9,10] The experimental uncertainty amounts to $\pm 15\%$.

TPA, as already observed for other quadrupolar systems and predicted by calculations.^[7a, 12, 13]

The nature of the conjugated chain also plays a crucial role. We note that although fluorophore **4** is slightly shorter than fluorophore **5**, it still shows a slightly higher TPA cross section at 740 nm (Table 1), seemingly correlated with the lower aromaticity of the thienyl ring and the concomitant lower energy cost associated with intramolecular charge transfer.^[12] This effect is, however, counterbalanced by a significant decrease in the quantum fluorescence yield. Consequently, fluorophore **4** shows a significantly smaller TPEF action cross section than does fluorophore **5** in the visible red region. Nonetheless, fluorophore **4** becomes more effective in the NIR region ($\lambda > 850$ nm), owing to a combined broadening and red shift of the TPEF spectrum (Figure 2a).

The TPA characteristics of the bis-donor fluorophores can also be strongly affected by the molecular environment, as indicated by the different behavior of fluorophore **5** in toluene and chloroform (Table 1). Its TPA cross section is almost 50 % larger in the more polar solvent, probably correlated with a stabilization of the intramolecular charge transfer. This underlines the influence of the environmental parameters on the TPA responses of quadrupolar fluorophores, as was the case for the quadratic nonlinear optical responses of dipolar chromophores.

Finally, the potential applications of these novel fluorophores for the imaging of biological membranes has been investigated by designing derivatives that combine the TPEF features of fluorophore **3** and slightly amphiphilic features (i.e. an extended hydrophobic central part and two hydrophilic end groups). The incorporation of fluorophore **12** in a model membrane of giant unilamellar vesicles made up of pure lipid in water can be imaged by TPEF microscopy (Figure 3).

Multiphoton microscopy is currently a blooming field, owing to the advantages it provides in biological imaging. Besides the ongoing development of optical systems, the design of novel fluorophores with optimized characteristics is of timely importance. This calls for the development of new molecular systems and the determination of general structure–property relationships, an approach that has already proved successful for quadratic nonlinear optics but is only emerging in the field of multiphoton absorption. The novel series of push–push fluorophores derived from an extended dihydrophenanthrene core actually demonstrates large TPEF cross sections in the visible-red or NIR region, a spectral window of particular interest for the imaging of biological tissues. Furthermore, by adjusting the length and nature of the conjugated extensor, both amplification and spectral tuning of TPA cross sections can be obtained. The enhanced performance of these molecules promises to be of particular importance in biological imaging applications.

Experimental Section

The TPEF excitation spectra of molecules **3–6** were measured according to the experimental protocol established by Xu and Webb,^[9] by using a mode-locked Ti:sapphire laser that delivers 80-fs pulses at 80 MHz. The quadratic dependence of the fluorescence intensity on the excitation intensity was verified for every data point, indicating that our measurements were

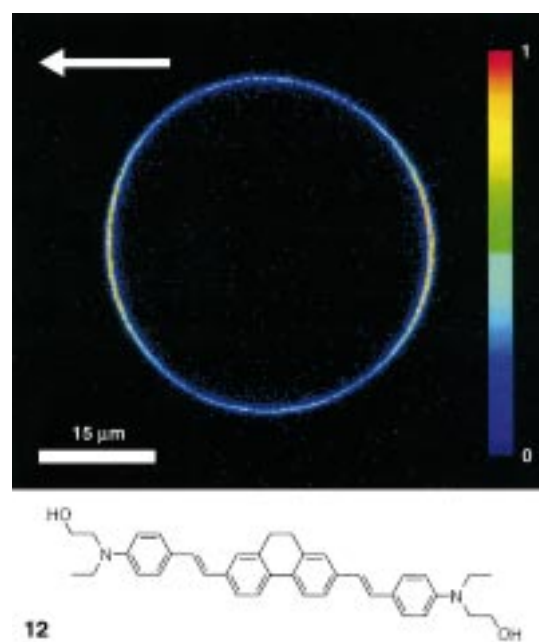


Figure 3. TPEF image of a giant unilamellar vesicle labeled with fluorophore **12**, excited at 750 nm with less than 1-mW excitation power. The vesicles were prepared from 1,2-dioleoyl-sn-glycero-3-phosphocholine (DOPC) and externally perfused with 40 μ M of fluorophore **12** in DMSO by using a protocol similar to that used in ref. [14]. Fluorescence anisotropy is observed when using a linearly polarized beam and selecting the corresponding parallel component of TPEF radiation (directed along the white arrow). This suggests a preferential transmembrane incorporation of derivative **12** whose total length approximately matches the width of the DOPC bilayer at room temperature.

carried out in intensity regimes in which saturation or photodegradation of fluorophores did not occur.

Received: January 2, 2001 [Z16360]

- [1] M. Göppert-Mayer, *Ann. Phys. (Leipzig)* **1931**, 9, 273–294.
- [2] D. A. Parthenopoulos, P. M. Rentzepis, *Science* **1989**, 245, 842–845; J. H. Strickler, W. W. Webb, *Opt. Lett.* **1991**, 16, 1780–1782.
- [3] a) G. S. He, G. C. Xu, P. N. Prasad, B. A. Reinhardt, J. C. Bhatt, A. G. Dillard, *Opt. Lett.* **1995**, 20, 435–437; b) J. E. Ehrlich, X. L. Wu, I.-Y. S. Lee, Z.-Y. Hu, H. Röckel, S. R. Marder, J. W. Perry, *Opt. Lett.* **1997**, 22, 1843–1845.
- [4] B. H. Cumpston, S. P. Ananthavel, S. Barlow, D. L. Dyer, J. E. Ehrlich, L. L. Erskine, A. A. Heikal, S. M. Kuebler, I.-Y. S. Lee, D. McCord-Maughon, J. Qin, H. Röckel, M. Rumi, X.-L. Wu, S. R. Marder, J. W. Perry, *Nature* **1999**, 398, 51–54.
- [5] a) W. Denk, J. H. Strickler, W. W. Webb, *Science* **1990**, 248, 73–76; b) C. Xu, W. Zipfel, J. B. Shear, R. M. Williams, W. W. Webb, *Proc. Natl. Acad. Sci. USA* **1996**, 93, 10763–10768, and references therein.
- [6] a) L. Ventelon, L. Moreaux, J. Mertz, M. Blanchard-Desce, *Chem. Commun.* **1999**, 2055–2056; b) J. W. Perry, S. Barlow, J. E. Ehrlich, A. A. Heikal, Z.-Y. Hu, I.-Y. S. Lee, K. Mansour, S. R. Marder, H. Röckel, M. Rumi, S. Thayumanavan, X.-L. Wu, *Nonlinear Opt.* **1999**, 21, 225–243; c) M. Rumi, J. E. Ehrlich, A. A. Heikal, J. W. Perry, S. Barlow, Z.-Y. Hu, D. McCord-Maughon, H. Röckel, S. Thayumanavan, S. R. Marder, D. Beljonne, J.-L. Brédas, *J. Am. Chem. Soc.* **2000**, 122, 9500–9510; d) O.-K. Kim, K.-S. Lee, H. Y. Woo, K.-S. Kim, G. S. He, J. Swiatkiewicz, P. N. Prasad, *Chem. Mater.* **2000**, 12, 2838–2841.
- [7] a) M. Albota, D. Beljonne, J.-L. Brédas, J. E. Ehrlich, J.-Y. Fu, A. A. Haeikal, S. E. Hess, T. Kogej, M. D. Levin, S. R. Marder, D. McCord-Maughon, J. W. Perry, H. Röckel, M. Rumi, G. Subramaniam, W. W. Webb, X.-L. Wu, C. Xu, *Science* **1998**, 281, 1653–1656; b) B. A.

Reinhardt, L. L. Brott, S. J. Clarson, A. G. Dillard, J. C. Bhatt, R. Kannan, L. Yuan, G. S. He, P. N. Prasad, *Chem. Mater.* **1998**, *10*, 1863–1874.

- [8] A. Helms, D. Heiler, G. McLendon, *J. Am. Chem. Soc.* **1992**, *114*, 6227–6238.
 [9] C. Xu, W. W. Webb, *J. Opt. Soc. Am. B* **1996**, *13*, 481–491.
 [10] M. A. Albota, C. Xu, W. W. Webb, *Appl. Opt.* **1998**, *37*, 7352–7356.
 [11] J. N. Derras, G. A. Crosby, *J. Phys. Chem.* **1971**, *75*, 991–1024.
 [12] M. Barzoukas, M. Blanchard-Desce, *J. Chem. Phys.* **2000**, *113*, 3951–3959.
 [13] W.-H. Lee, M. Cho, S.-J. Jeon, B. R. Cho, *J. Phys. Chem. A* **2000**, *104*, 11 033–11 040.
 [14] L. Moreaux, O. Sandre, M. Blanchard-Desce, J. Mertz, *Opt. Lett.* **2000**, *25*, 320–322, 678.

Remote Stereocontrol in Carbonyl Additions Promoted by Vinylstannanes**

Asunción Barbero, Francisco J. Pulido,*
 Juan A. Rincón, Purificación Cuadrado,
 Diego Galisteo, and Henar Martínez-García

The search for highly stereocontrolled routes for the preparation of chiral compounds is an important goal in organic chemistry.^[1, 2] The asymmetric addition of nucleophiles to carbonyl groups is a cornerstone of organic synthesis and as such has been extensively reviewed.^[3] Although asymmetric induction by stereogenic centers adjacent to carbonyl groups has been widely studied, more remote inductions are less well known.^[1–3]

Thomas and co-workers reported the potential of the allylstannane moiety in the construction of chiral compounds, and showed many examples of remote asymmetric induction by allylic tin reagents and oxocompounds.^[4] Other outstanding reactions that involve chiral allylstannanes were reviewed by Marshall.^[5]

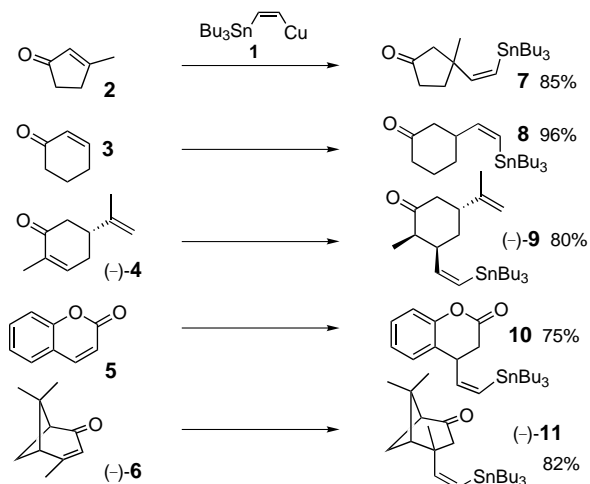
Herein we report a highly efficient stereocontrolled addition of organometallic reagents to carbonyl groups in the presence of a (*Z*)- β -stannylvinyl group. The remote stannyl group induces a highly stereoselective attack from the same face on which the tin center is found. To the best of our knowledge, the long-distance control effected by the vinyltin moiety has not been observed before. The role of the tin center, the influence of the Sn–CO bond separation, and a hypothetical mechanistic pathway that leads to this remarkable stereocontrol are discussed herein.

[*] Dr. F. J. Pulido, Dr. A. Barbero, Dr. J. A. Rincón, Dr. P. Cuadrado, Dr. D. Galisteo, Dr. H. Martínez-García
 Departamento de Química Orgánica, Universidad de Valladolid
 47011 Valladolid (Spain)
 Fax: (+34) 983-423013
 E-mail: pulido@qo.uva.es

[**] We Thank the M.E.C. of Spain (PB96/0357) and the Junta de Castilla y León (VA43/98) for financial support. We are very much indebted to Dr. Santiago García-Granda, Oviedo (Spain) for X-ray crystallographic assistance.

The introduction of a vinylstannyl unit β to a carbonyl group was achieved by stannylcupration of acetylene, followed by treatment with α,β -unsaturated ketones. The stannylcupration of allenes^[6] and acetylenes^[7] has emerged as an important tool in the synthesis of allyl- and vinylstannanes.^[8, 9]

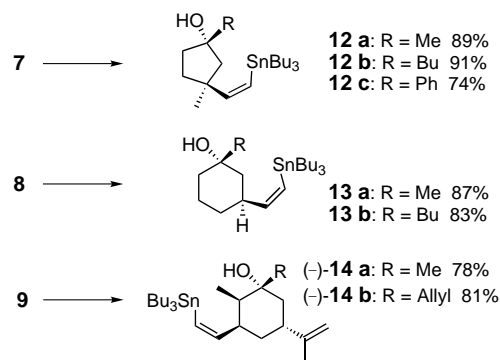
cis-2-(Tributylstannyl)vinyl cyanocuprates **1**^[7] react with enones **2–6** to give, after conjugate addition, *cis*- β -(tributylstannyl)vinyl ketones **7–11** in good yield (Scheme 1). The



Scheme 1. Reaction of enones **2–6** with cuprate **1**. Reagents and conditions: 1) **1** (1.0 equivalent), BF₃·Et₂O, THF, –78 °C, 30 min; 2) –78 → 0 °C, 1 h; 3) NH₄Cl/H₂O, 0 °C.

addition of one to two equivalents of BF₃ to the cuprate prior to the addition to the ketone increases the final yield significantly.^[10] *(-)*-(5*R*)-Carvone (**4**) and *(-)*-(1*S*,5*S*)-verbenone (**6**) underwent stereoselective conjugate addition to give the optically active ketones (2*R*,3*R*,5*R*)-**9** and (1*S*,4*S*,5*R*)-**11**, respectively.^[11a]

The behavior of **7–9** toward typical organolithium reagents shows that addition occurs with a high degree of stereocontrol. The reaction of **7–9** with MeLi, BuLi, allyllithium, and PhLi in THF at –78 °C affords diastereoselectively the tertiary alcohols **12–14** (Scheme 2), respectively, in which the addition of the alkyl or phenyl groups takes place *syn* to the



Scheme 2. Stereoselective addition of organolithium reagents to β -stannylvinyl ketones **7**, **8**, and **9**. Reagents and conditions: 1) RLi (1.2 equivalents), THF, –78 °C, 30 min; 2) MeOH, –78 °C.